Spontaneous Growth of Two-Dimensional Complex Patterns of Nanoparticles at Model Molecular Surfaces

ARTICLE *in* LANGMUIR · JANUARY 2001

Impact Factor: 4.46 · DOI: 10.1021/la0012034

3 AUTHORS, INCLUDING:

Dr. Hamidou Haidara
French National Centre for Scientific Research
85 PUBLICATIONS **469** CITATIONS
SEE PROFILE

Karine Mougin
French National Centre for Scientific Research
35 PUBLICATIONS **354** CITATIONS
SEE PROFILE

Research Article

Spontaneous Growth of Two-Dimensional Complex Patterns of Nanoparticles at Model Molecular Surfaces

H. Haidara, K. Mougin, and J. Schultz

Langmuir, **2001**, 17 (3), 659-663 • DOI: 10.1021/la0012034

Spontaneous Growth of Two-Dimensional Complex Patterns of Nanoparticles at Model Molecular Surfaces

H. Haidara,* K. Mougin, and J. Schultz

Institut de Chimie des surfaces et Interfaces, Centre National de la Recherche Scientifique, 15 Rue Jean Starcky, B.P. 2488, 68057 Mulhouse Cedex, France

Received August 21, 2000. In Final Form: October 12, 2000

Imposed anisotropy of either physical or geometrical origin is known to be a determining parameter in the emergence of complex patterns (fractals, dendrites) in organizing matter (crystallization, growth of bacterial colonies). In such systems, any local gradient in a physicochemical parameter or broken symmetry may result in complex growth shapes. In contrast, the formation of self-organized complex patterns at, say, molecularly smooth and chemically homogeneous surfaces in a uniform and structureless solution of monosized particles constitutes a rare and incompletely explored phenomenon. We here report on such spontaneous emergence of two-dimensional treelike patterns of nanogold particles that are adsorbed from aqueous dispersions, at both homogeneous and mixed self-assembled molecular surfaces. These results provide a new picture on the connection between wetting dynamics, interface instabilities, and the spontaneous formation of complex patterns at chemically homogeneous and anisotropy-free surfaces. In the specific case of nanogold particles, these results may have important applications in biology and nanoscience.

Introduction

How can complex aggregation morphologies such as arborescent (multibranched) patterns emerge from the aggregation of monosized colloidal particles, at a *uniform and anisotropy-free* surface? Which mechanism is involved and which parameters are critical for the control of the growth pattern in such phenomena, which are known to be essential in generating new properties and behavior[1−4]in both living and nonliving matter? For instance, bacterial colonies have been shown to spontaneously grow in complex aggregation morphologies,[1] whose topological features are determined by the local environmental conditions (chemotacticity, gradients in nutrients, etc.). In the same way, crystallization of proteins at a substrate may also result in complex aggregation patterns, depending on the specific properties of the surface−solution interface. The understanding of the underlying mechanisms that drive the emergence of these complex aggregation patterns is therefore of particular importance and is essential in biology.[1] So also is the case in material science (metallurgy, electrochemistry, colloids, etc.), where such complex patterns can form in both bulk[2] (solidification) and interface systems[3,4] (colloids), leading to specific conduction (heat or electrical) properties or mechanical behavior. In the growing field of nanoscience,[3,5] and more specifically, for 2-D aggregation structures of nanometal particles, the ultimate physical properties (electromagnetic, for instance) of the colloidal network are known to strongly depend on their topology. The search for optimal conditions leading to the formation of complex aggregation clusters, spanning hundreds of micrometers, may significantly contribute to the understanding of this topology-dependent behavior, through direct experimental investigations on large-scale single clusters.

The conditions under which the complex patterns are formed in these investigations are quite specific (uniform and anisotropy-free surface, homogeneous and monosized colloidal dispersion) as compared to standard conditions where they usually emerge, either driven by[1,2,4] local anisotropy, phase separation, local gradient in physicochemical parameters, or externally induced fluid flow. We here used model molecular surfaces and aqueous dispersions of nanogold particles (diameter ∼ 25 nm), to investigate the formation of these complex multibranched patterns that can grow to sizes spanning hundreds of micrometers. These results are then discussed and a tentative phenomenological model, based on existing works in this domain, is proposed for the growth mechanisms of these complex aggregation morphologies.

Experimental Section

We used fresh aqueous dispersions of nanogold particles ($HAuCl_4$), stabilized with small anionic citric acid trisodium salt dihydrate molecules.[6] The characteristic size of the nanogold particles was 25 ± 5 nm, as determined from atomic force microscopy (AFM) topographic images. The model surfaces were molecular films of alkylsilane compounds, self-assembled onto silicon wafers. Two organosilane compounds, the hexadecyltrichlorosilane $Cl_3Si(CH_2)_{15}CH_3$ and (6-aminohexyl)aminopropyltrimethoxysilane $(OCH_3)_3$-$Si(CH_2)_3$-NH-$(CH_2)_6$-NH_2, were used to elaborate (i) two uniform and molecularly smooth amine- and methyl-terminated surfaces (respectively referred to as RNH_2 and RCH_3) and (ii) a heterogeneous surface (referred to as CH_3/NH_2), composed of the distribution of RCH_3 nanodomains within the continuum of RNH_2 molecular film (Figure 1). Both the organosilane compounds and nanogold particles were from ABCR, Karlsruhe, Germany, whereas the trisodium citric acid was from Aldrich. The heterogeneous binary surfaces were elaborated based on the well-established experimental fact that solvent-coated organosilane films self-assembled onto silicon wafers initially grow up as isolated nanoislands, before they touch to form a continuous and well-packed monolayer.[7] By the unique

* Corresponding author: e-mail h.haidara@univ-mulhouse.fr; phone (33) 03 89 60 87 67; fax (33) 03 89 60 87 99.

(1) Ben-Jacob, E.; Sochet, O.; Tenenbaum, A.; Cohen, I.; Cziròk, A.; Vicsek, T. *Phys. Rev. Lett.* **1996**, *53*, 1835.
(2) Langer, J. S. *Rev. Mod. Phys.* **1980**, *52*, 1.
(3) Shipway, A. N.; Katz, E.; Willner, I. *ChemPhysChem*. **2000**, *1*, 18.
(4) Yeh, S.-R.; Seul, M.; Shraiman, B. I. *Nature* **1997**, *386*, 57.
(5) Martin, C. R.; Mitchell, D. T. *Anal. Chem. News Features* **1998**, *May 1*, 322A.
(6) Kunz, M. S.; Shull, K. R.; Kellock, A. J. *J. Colloid Interface Sci.* **1993**, *156*, 240.

10.1021/la0012034 CCC: $20.00
Published on Web 01/09/2001

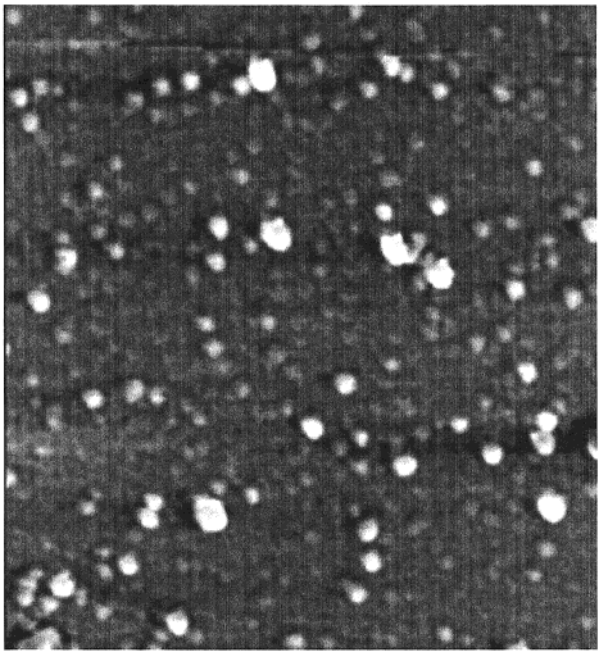

Figure 1. AFM picture of the nanoheterogeneous (RCH_3/RNH_2) molecular surface. Methyl- (RCH_3-) terminated nanodomains (nodes) are distributed within the amine- (RNH_2-) terminated continuum (background). The average thickness difference ("roughness") between RCH_3 nanodomains and background amine NH_2 continuum = 1 nm.

control of the adsorption time for a given concentration and temperature of the organosilane solution, isolated RCH_3 nanoislands could be produced on the virgin wafer. These nanodomain-coated samples were thoroughly rinsed with pure solvent to remove free and loosely adsorbed molecules and then dried under nitrogen. The complete heterogeneous binary molecular surfaces were obtained from the nanodomain-coated samples by immediately adsorbing the continuous molecular phase (RNH_2) in the remaining free space of the silicon substrate by solvent deposition. A more complete description of both the surface preparation and elaboration process of self-assembled nanoheterogeneous surfaces can be found in a related recent work.[7] It is worth mentioning here that the typical roughness at these nanoheterogeneous surfaces, which mainly arises from the difference in the thickness of the two molecular phases (respectively 1 and 2 nm for the NH_2 and CH_3 domains), lies in the subnanometer range, as estimated by both ellipsometry and AFM. Since this nanometer-scale "roughness" is known to have a negligible effect (if any) in interface phenomena (wetting, hysteresis), the predominant effect one expects from these surface structures is that arising mainly from the nanoscale compositional heterogeneity. To confirm this compositional heterogeneity at the molecular scale, we performed a two-step analysis on both CH_3 nanodomain-coated virgin wafers and final heterogeneous binary CH_3/NH_2 surfaces, using both X-ray photoelectron and infrared (IRRAS) spectroscopy.[7] These analyses, respectively based on Si−C bonds for the CH_3 domains onto the virgin wafer and Si−C and C−H bonds for the heterogeneous CH_3/NH_2, have clearly revealed the presence of the two molecular phases, as shown in Figure 1. The advancing and receding contact angles of water on these substrates (θ_a, θ_r) were, respectively, (87°, 56°) for heterogeneous CH_3/NH_2 surfaces and (59°, 21°) for uniform RNH_2. The substrates were either allowed to support a drying drop of the dispersion, while placed under a microscope where the drying and pattern formation were recorded by use of a videocamera device, or immersed in the suspension for different times. In this latter case, which we mainly used for these

(7) Haidara, H.; Mougin, K.; Schultz, J. *Langmuir* **2000**, *16*, 7773.

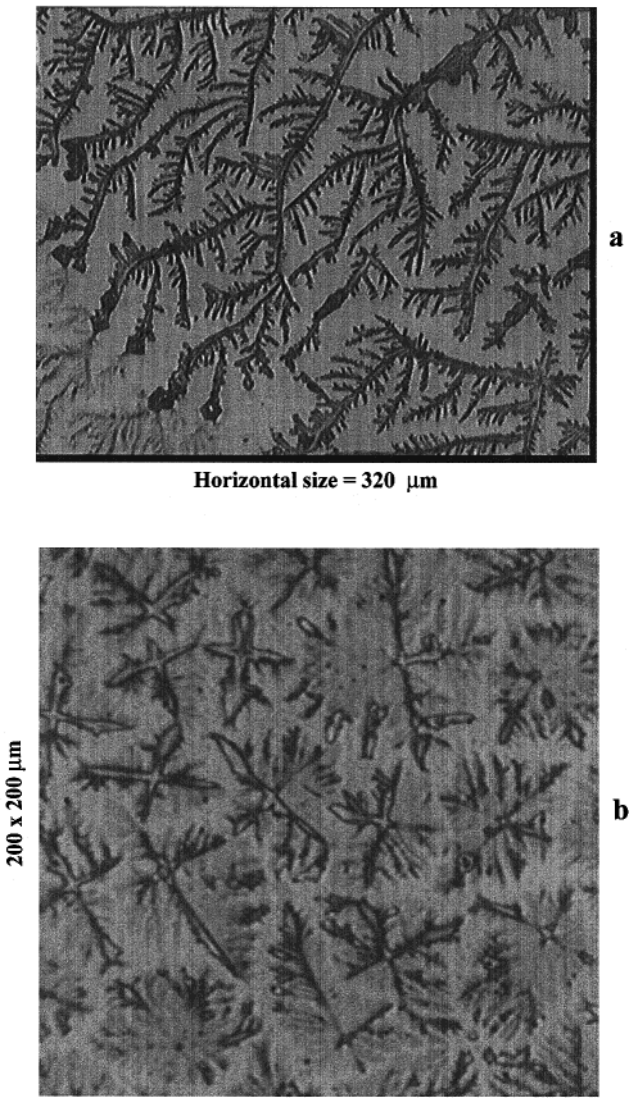

Figure 2. Drying patterns formed upon 0.5 h of preadsorption in an aqueous suspension containing 0.03 wt % nanogold particles. (a) Complex aggregation pattern at the uniform amine- (RNH_2-) terminated surface. (b) Fourfold dendritelike pattern at the nanoheterogeneous (RCH_3/RNH_2) surface.

experiments, the thick dispersion drop (pancake) remaining at the emerged substrate is then allowed to dry, under the same conditions as the deposited drops. An additional advantage of this method is that it allows us to study the influence of the surface fraction of adsorbed particles on the characteristic features of the late-stage-emerging patterns. Unless specified, all the experiments, especially the drying of the deposited drop, were performed at the ambient temperature (~22 °C) and the typical dispersion concentration c used was 0.03 wt %. The aggregation patterns corresponding to an adsorption time of 0.5 h at the featureless NH_2 and nanoheterogeneous CH_3/NH_2 surfaces are represented, respectively, in panels a and b of Figure 2. The most striking feature of concern here is the higher complexity of the large (few hundreds of micrometers) multibranched patterns that form at molecularly smooth and chemically homogeneous hydrophilic RNH_2 surfaces, as compared to the randomly oriented 4-fold dendrites at heterogeneous CH_3/NH_2 surfaces.

Results and Discussion

On the basis of the quite well understood growth mechanism and selection rule for dendrites (anisotropy for main branches and perturbation along them for side ones),[1,2] one can preclude (in a uniform dispersion) the

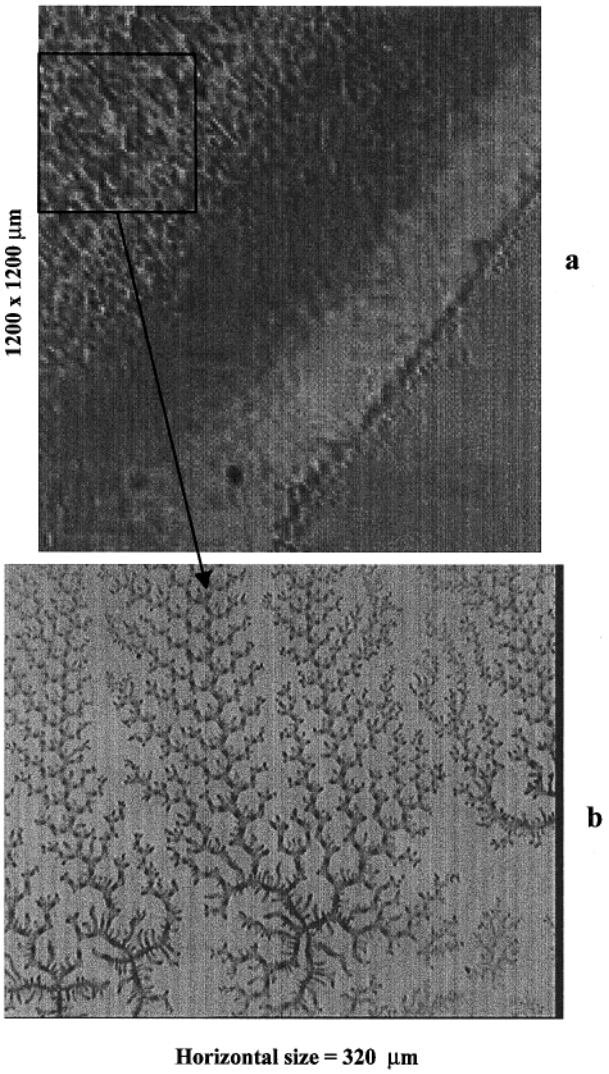

Figure 3. Snapshots of the periphery of the drying drop showing the growth mechanism of the complex patterns at the amine-terminated surface. (a) The structures form within the wetting film as the fluid recedes from the periphery. (b) Magnification showing the detail of the shear-stretched patterns appearing at the wetting film periphery.

emergence of such patterns at surfaces that are *homogeneous and isotropic* at any scale (for NH_2), or at least, at scales $\lambda \sim 1$ μm (for CH_3/NH_2, Figure 1). This is well supported by the experiments, where the complex patterns appear exclusively during the free drying and shrinking of the dispersion drop (Figure 3). The hydrodynamic effects (drainage, instability)[8,9]involved in this late-stage drying are thereafter considered to account for the redistribution of the particles at the interface and the emergence of the observed morphologies. A critical boundary condition in this drying process is the extent of the contact line pinning, which depends on the receding contact angle θ_r of the solvent drop with the substrate. This controls the peripheral drainage of the drop liquid and particles as well as the friction, τ, upon the collected particles in the wedge, as the drop starts to shrink at some θ_r. For substrates presenting large receding contact angles θ_r (partial to nonwetting), this mechanism[8,9] often results in the formation of a peripheral aggregation ring. That was predicted by a power-law time growth of the particles in the wedge, $M(r,t) - M_0(R,t_0) \sim (t - t_0)^p$, in good agreement with experiments.[8] In contrast, at receding angles close to zero ($\theta_r \ll 1$ rad), where a higher particle-substrate sticking coefficient σ is expected, the growth pattern at the surface might be dominated by the friction at the leading edge between the collected particles within the moving wedge (velocity v, thickness h) and those strongly attached (layered)[8,9] at the interface: $\tau_w \sim \eta(v/h)|_{wedge}$. These conditions at the contact line were satisfied only at NH_2 substrates ($\theta_r \sim 0.4$ rad), whereas the drying drop continuously thins down to zero at fixed contact area (complete pinning) at strong hydrophilic substrates (clean silanol-enriched silicon plates, for instance), resulting in randomly distributed coarse dendrite aggregates. At retracting contact angles $\theta_r \geq 1$ rad, one expects the local thickness h_w, retracting velocity v, and particle density at the wedge all to be higher, as observed experimentally ($v_{CH_3} \sim 2v_{NH_2}$ for drying drops deposited on these surfaces at 22 °C). At these less wettable surfaces (CH_3, CH_3/NH_2), which equally exhibit a lower particle sticking coefficient σ (higher interface slippage), the magnitude of the shear stress decreases as $h_w^{*-1} = (h_w + b)^{-1}$, where h_w^* is the augmented wedge thickness by the slippage length[10] b, and $l_w(tg\theta_r) \sim h_w$, the first-order functional dependence between the retracting angle θ_r, the characteristic length l_w, and height h_w of the wedge.[10] The magnitude of the shear-induced orientation within the wedge particles finally scales as

$$\tau_w \sim \eta v h_w^{*-1} \sim \eta v[(l_w tg\theta_r) + b]^{-1} \qquad (1)$$

To leading order, the pattern formation in this process is thus determined by the wetting dynamic (θ_r) and surface chemistry [$\sigma \sim (1 + b)^{-1}$], which in turn govern the hydrodynamic within the retracting wedge (inward flow, shear-induced redistribution, and ordering of particles). This phenomenological description is well supported by the highly stretched treelike patterns, which appear within the thin wetting film at the periphery of the drop (Figure 3), as the fluid periodically (in the manner of a stick−slip event) recedes from this wetting film. The influence of the surface chemistry (sticking σ) as a critical condition for the emergence of the multibranched pattern (Figure 2a) was demonstrated through different dwell times. Whereas an immersion time of 15 min is sufficient to develop the arborescent patterns at the uniform NH_2 surface, a minimum of 1 h is required for the heterogeneous binary CH_3/NH_2 surface. This difference actually accounts for the extent of two distinct phenomena, both related to the dwell time: the interface conversion and the amount of aqueous dispersion entrained along with the emerged substrate. For the uniform R-NH_2 substrate, the surface modification leads to the formation of a first close-packed and strongly attached monolayer of nanogold particles as revealed by AFM observations, on top of which less well-packed and loosely attached layers may grow. One has used a simple mechanical test (10 s sonication) to successfully assess the adhesion of this first two-dimensional array, which can strongly attach to the amine surface, through either hydrogen or electrostatic bonds between the surface groups (NH_2, NH_3^+) and the stabilizing citrate anions R-COO- at the nanoparticle surface. As a result of that full conversion, which substitutes a highly hydrophilic 2-D array (or multilayer) of charged Au-COO- particles for NH_2 groups, a thick wetting film (pancake)

(8) Deegan, R. D.; Bagajin, O.; Dupont, T. F.; Huber, G.; Nagel, S. R.; Witten, T. A. *Nature* **1997**, *389*, 827.
(9) Parisse, F.; Allain, C. *Langmuir* **1997**, *13*, 3598.
(10) de Gennes, P. G. *Rev. Mod. Phys.* **1985**, *57*, 827.
(11) Sun, L.; Crooks, R. M.; Ricco, A. J. *Langmuir* **1993**, *9*, 1775.

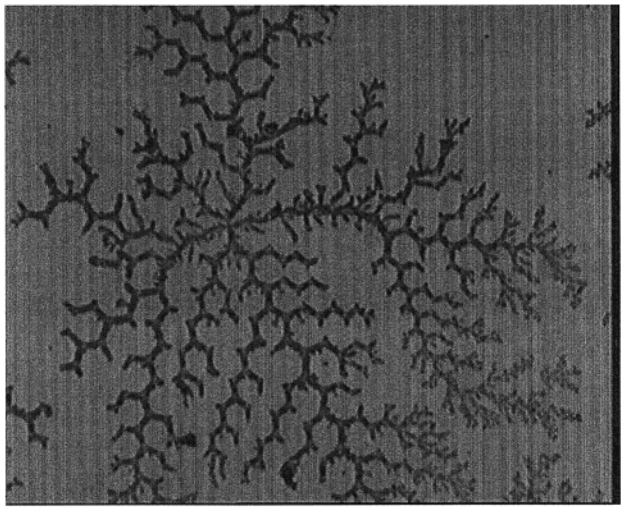

Figure 4. A few of the more symmetrical aggregation patterns formed at amine-terminated surface at longer preadsorption times in the aqueous suspension (1−4 h).

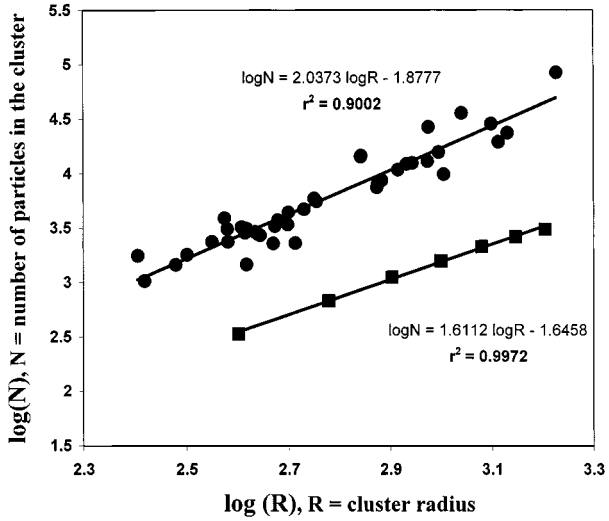

Figure 5. Number of particles vs cluster size (radius) plots (log N vs log R): (■) highly stretched anisotropic clusters as shown in Figure 3b, (●) more symmetrical clusters as shown in Figure 4. The fractal dimensions were, respectively, $D = 1.61$, $R^2 = 0.997$ for the highly stretched structures (average over 8 clusters), and $D = 2.03$, $R^2 = 0.900$ for the more symmetrical ones (average over ∼35 clusters).

is entrained by the uniform amine surface. It then seems that the drainage within the less well-packed and loosely attached particles in the top layers at the uniform RHN_2 substrates contributes in a determining way to the formation of the complex aggregation patterns at these surfaces. In contrast, a less packed and irregular Au-COO-particle array is formed at the heterogeneous CH_3/NH_2 surface, where hydrophobic RCH_3 domains represent nonattaching defects within the RNH_3^+ continuum. For equivalent dwell times, a thinner pancake is thus entrained along with this rough and less hydrophilic surface, as compared to the uniform RNH_3 substrate. At fixed substrate area, this thickness difference results in a difference in the number of particles ΔN at the two interfaces, which was estimated by weighing to be $\sim 10^{10}$ particles, by use of $c = 0.03$ wt % and the average particle volume. Both the surface and dwell-time dependence of the growth patterns (arborescent or 4-fold dendrites) then seem to be related to some critical amount of particles N_c in the drying suspension (reservoir). The wetting and interface properties of the two substrates are such that N_c is achieved over short dwell times for the emergence of multibranched patterns on RHN_2 substrates, whereas large time scales are required at CH_3/NH_2 substrates to achieve the transition from dendritelike to arborescent patterns. Though the highly stretched clusters (Figure 3b) represented the aggregation structure, whose formation could be easily located and observed during the experiment, the drying spot also contains both intermediate and more symmetrical multibranched patterns (Figure 4), which appear behind the triple line during its regular retracting motion. To determine whether these complex structures were fractal, we have chosen the two extreme populations of aggregation clusters: the highly stretched, anisotropic patterns (Figure 3b) and the more symmetrical ones (Figure 4). The fractal plots made on each of these two populations, by use of the number−radius relation[12,13] on both subsets, boxes and entire clusters, have led to two characteristic dimensions. The more symmetrical aggregates, despite their striking resemblance to 2-D clusters produced in a diffusion-limited aggregation (DLA) model,[14] were found to possess the trivial Hausdorff fractal dimension[13] of the space (plane), $D = 2.03$ (Figure 5). Though surprising owing to their open structure, this result is not singular, such patterns being predicted and expected from simulations based on ballistically driven aggregation models.[13] The highly stretched anisotropic clusters were found to be fractal with a dimension $D \sim 1.61$ (Figure 5), which is reminiscent of a diffusion-limited aggregation (DLA) mechanism. Between these two extreme aggregation topologies, no unique fractal property was found for the population of intermediate aggregation topologies, their fractal dimension varying from $D = 1$ to 1.4, dependent on which ensemble of intermediate aggregation topology was selected.

Finally, the central role played by both the hydrodynamic effects and the underlying particle array in the emergence of the complex patterns seem to suggest their analogy with viscous fingering in 2-D porous media.[14] In this model, the critical parameters, which drive the formation of the fingers, are the velocity of the moving fluid−fluid interface in the referential of the 2-D porous bed, the packing density of the porous medium, and the relative viscosity of the fluids (invading/resisting fluids). In our system, the aqueous dispersion of higher viscosity recedes over the surface, pushed by the surrounding air at a velocity v through 2-D connected channels of the porous bed, which constitute preferential flow lines. Particles may then be drained from these streamlines and collected between them in well-organized complex patterns. In comparison with the standard 2-D Hele-Shaw experiment with a horizontal cell (gravity $g \approx 0$),[14] this is equivalent to the fluid (drop) being sucked off at an average velocity $v = -\mu\nabla P$, where μ, the ratio of the bed's permeability to the viscosity of the fluid, represents the fluid mobility through the porous medium. For the drying drop, the pressure gradient at the receding wedge $\nabla P = [P(\text{outside drop}) - P(\text{inside})]$ roughly amounts to the disjoining pressure term Π of the wetting film,[15] irrespective of the magnitude of the Laplace pressure term, $2\gamma\kappa$,

(12) Hwang, R. Q.; Schröder, J.; Günther, C.; Behm, R. J. *Phys. Rev. Lett.* **1991**, *67*, 3279.
(13) Bensimon, D.; Shraiman, B.; Liang, S. *Phys. Lett.* **1984**, *102A*, 238.
(14) Feder, J. *Fractals*; Plenum Press: New York, 1998; p 42.
(15) Churaev, N. V. *J. Colloid Interface Sci.* **1995**, *172*, 479.

which depends on the local curvature κ at the wetting film−drop transition and the fluid interface tension γ. At first order, this leads to a velocity of the fluid front $v \sim -\mu\Pi$, and hence, a friction term within the wedge:

$$\tau_w \sim -\eta\mu\Pi[(l_w tg\theta_r) + b]^{-1} \quad (2)$$

which definitely shows how wetting properties at the substrate/dispersion interface and the particle aggregation state at the substrate dominate the formation of the complex patterns in these dynamics. Interestingly, the unique specific feature of our system as compared to existing patterns produced in Hele-Shaw cells during the displacement of a fluid−fluid front in 2-D porous media is the relative mobility of the particle array, which may appear under shear. This internal freedom of the particles in the 2-D porous media may strongly affect the overall growth process and, thus, the characteristic features of the emerging patterns.

These results well demonstrate the drastic influence *nanoscale* compositional heterogeneity may have on interface phenomena, which at first insight are driven by macroscopic processes (wetting and hydrodynamics). The total absence of length-scale correlation between the aggregation patterns (∼hundreds of micrometers) and the underlying surface structures (domain size and distance ∼ 50 nm) at the nanoheterogeneous surface (RCH_3/NH_2) clearly indicates that one may neglect any discrete contribution from the nanodomains in the emergence of these aggregation patterns. This conclusion was confirmed in recent studies[16] where AFM observations revealed the absence of any discrete effect (epitaxy or templatelike growth) of the underlying nanodomains that could be observed in the "monolayer" structure at the substrates, as long as their size remains less than or approximately equal to the particle size. Though one could intuitively expect this result, this work definitely provides an experimental basis, which may serve for further theoretical investigations of nanoscale effects in interface phenomena.

(16) Haidara, H.; Mougin, K.; Schultz, J. *Langmuir* (submitted for publication).

Conclusion

These results have revealed a very particular class of spontaneous pattern formation in nanosized colloidal systems, which adds to the diversity of existing growth mechanisms and models. The growth mechanisms are shown here to be governed primarily by the "substrate-dispersion" wetting properties. It was then possible, by simply adjusting the top surface chemistry and composition of the substrate, to generate a diversity of aggregation morphology and size. These results may provide a new picture toward the complete understanding of the 2-D self-organization and complex pattern formation in both living and nonliving systems, as they open an attractive route for the controlled growth of 2-D networks for nanophysics and biology. For instance, each of these single aggregation clusters, as shown in Figures 3b and 4, may serve as a potential model in studying the dependence of the electromagnetic properties of an object (2-D or 3-D network) on its intrinsic topological features.

Acknowledgment. We thank G. Castelein for initiating one of us (K.M.) to both the technique and treatment of atomic force microscopy (AFM) data. H.H. is especially grateful to N. Rivier for the interesting discussions we had in the early stage of this work, which were revealed later to be of considerable help.

LA0012034